

Settling of Drilling Cuttings in Polymeric Solutions: A Parametric Investigation

Arafat A. A. Mohammed, Mohammed Alhajabdalla, Husameldin Mahmoud, Mustafa S. Nasser,*
Ibnelwaleed A. Hussein, and Ramadan Ahmed

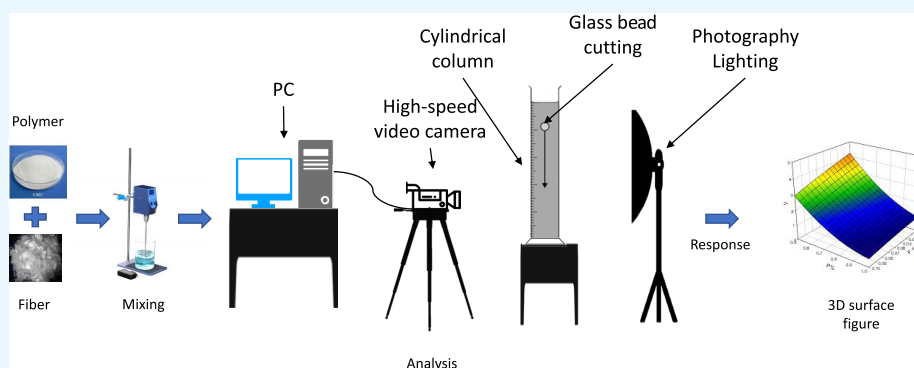
Cite This: *ACS Omega* 2023, 8, 21830–21841

Read Online

ACCESS |

Metrics & More

Article Recommendations



ABSTRACT: Drilling fluids, commonly referred to as drilling mud, are pumped into the wellbore to expedite the drilling process by moving drilling cuttings to the surface, suspending cuttings, controlling pressure, stabilizing exposed rock, and providing buoyancy, cooling, and lubrication. Understanding the settling of drilling cuttings in base fluids is crucial for successfully mixing drilling fluid additives. In this study, the response surface method Box–Behken design (BBD) is used to analyze the terminal velocity of the drilling cuttings in a polymeric base fluid of carboxymethyl cellulose (CMC). The impact of polymer concentration, fiber concentration, and cutting size on the terminal velocity of the cuttings is investigated. The BBD of the three factors (low, medium, and high) is used for two fiber aspect ratios (3 and 12 mm length). The size of the cuttings varied between 1 and 6 mm, while the concentration of CMC was between 0.49 and 1 wt %. The concentration of the fiber was in the range of 0.02–0.1 wt %. Minitab was utilized to determine the optimum conditions for reducing the terminal velocity of the suspended cuttings and then evaluate the effects and interactions of the components. The results show good agreement between model predictions and the experimental results ($R^2 = 0.97$). According to the sensitivity analysis, cutting size and polymer concentration are the most crucial factors affecting the terminal cutting velocity. Large cutting sizes have the most significant impact on polymer and fiber concentrations. The optimization results revealed that a CMC fluid with a viscosity of 630.4 cP is sufficient to maintain a minimum cutting terminal velocity of 0.234 cm/s with a cutting size of 1 mm and a 0.02 wt % of the 3 mm length fiber.

1. INTRODUCTION

Developing drilling fluid additives is still a critical challenge for enhancing the drilling process.¹ Drilling fluid or drilling mud is circulated in the borehole for efficient and cost-effective drilling operations.^{2–4} The drilling mud is composed of condensed liquids that can be synthetic or oil- or water-based and contain various heavy minerals and chemical additives pumped through the drilling pipe to carry out specific tasks.^{5,6}

Drilling fluids perform several crucial tasks, including transporting cuttings to the surface, well control, cooling, lubricating, and supporting a portion of the weight of the drill bit and drill pipe.^{7–11} The transport path of the cuttings is influenced by the well being drilled. Cuttings are moved from the borehole to the surface while drilling wells along the

horizontal, built-up, and vertical portions. Cuttings quickly settle down in the drilling fluid when drilling activities are stopped under specific conditions, such as the connection of the drill pipe. Cutting concentration in the vertical portion and cutting bed thickness in the deviated sections are both impacted by settling velocity.^{12,13} The chance that the cuttings may settle and the cuttings may bury the drill bit inside the wellbore increases if

Received: March 6, 2023

Accepted: May 25, 2023

Published: June 7, 2023



Table 1. Material Sources and Properties

Material/source	Properties
Carboxy Methyl Cellulose Sodium (CMC): - (Arshine pharmaceutical co. Ltd, Hunan, China) <div style="text-align: center;"> </div>	- CAS No.: 9004-32-4 - Molecular Weight: 242 g/mol - Purity: 99.5% (min)
Fibers (Virgin polypropylene): - (FORTA Super-Sweep, Pennsylvania, USA)	- Monofilament fibers - Specific Gravity: 0.9 - Length: 3.175 mm, 12.7 mm - Diameter: 100 μm - Environmental effect: LC50 value of 1 million, Safe
Glass Beads (Cuttings): - ISOLAB GmbH, Wertheim, Germany (3 & 6 mm) - YIWU SANJIA Electronic Commerce Co., Ltd. Zhejiang, China (1 mm)	- Spherical - Inert - Red color - Composition: Borosilicate - Diameter: 1, 3.5, & 6 mm - Specific Gravity: 2.4, 2.3, 2.5, for 1, 3.5, and 6 mm, respectively

the settling velocity is very high because the cutting bed or cutting plug will soon form in the deviated portions.^{14–17} In horizontal and deviated wells, efficient wellbore cleaning is crucial. It may avoid issues like stuck pipe, lost circulation, high torque and drag, and loss of control on equivalent circulation density (ECD). Lastly, it can lower the cost of the drilling operations.

Wellbore cleanout operation is the most widely used technique in horizontal and highly inclined wells. Due to several operational parameters, the process often involves complex and costly procedures. If not appropriately performed, some parts of the wellbore can be left uncleaned. The presence of solids in the wellbore causes several operational problems including pipe stuck, loss of circulation, drilling failures, borehole instability, mud contamination, and producing formation damage.^{18,19} The traditional method of improving hole cleanout operation performance is applying viscous pills or gelled sweeps (i.e., viscous fluids formulated for wellbore cleanout operation). Even though gelled sweeps effectively clean vertical wellbores, the performance is low in a well's highly deviated and horizontal sections. Their particle lifting capability in horizontal configuration is low. As a result, they are unable to suspend deposited particles.

Recently, many studies showed the use of drilling fluids that include fibrous materials to enhance wellbore cleaning and cutting suspension during the drilling operation.^{20–23} Field experiments show that fiber-containing sweep fluids may efficiently remove drill cuttings from wells that are horizontal and strongly inclined.¹¹ According to studies, cutting transport is influenced by cutting parameters, fluid parameters, operational factors, and formation parameters, with the fluid flow rate and rheology being the most tightly regulated characteristics.²⁴ The drilling fluid's flow regime and rheological characteristics are crucial factors in well-cleaning operations.²⁵ Adding fibers to the drilling fluids slows down the cutting settling velocity, and it can entirely suspend cuttings smaller than a threshold specified by the base fluid's characteristics and fiber content. This study aims to identify the optimum condition for the settling velocity of drilling cuttings in a fibrous carboxymethyl cellulose (CMC)

water-based fluid. Box–Behnken design (BBD) with four factors and three replicates are used to generate statistical models for optimizing the cutting terminal velocity and identifying its stability areas. The terminal velocity was investigated using three cutting sizes, three fiber concentrations, and two fiber lengths in a CMC water-based fluid of three concentrations. A cylindrical column, high-speed video camera, photography lighting, and a PC were used to run and record the experiments.

2. EXPERIMENTAL SETUP AND METHODS

2.1. Materials. White polypropylene monofilament synthetic fibers with a specific gravity of 0.91 and an average melting point of 172 °C (FORTA Super-Sweep fiber) were used in this study. Two types of these fibers are used with dimensions of 100 μm diameter and 3 and 12 mm length (concerning aspect ratios of 30 and 120, respectively). Carboxymethyl cellulose (CMC) polymers were used as base fluids with various concentrations. Inert glass beads with a size range of 1–6 mm were employed to mimic the actual drilling cuttings. Table 1 lists each material's sources and properties.

2.2. Fiber Stability. In the oil and gas business, fibers are widely employed as a fluid additive to boost hydraulic fracturing efficiency, decrease fluid filtration loss, and increase hole-cleaning performance. A small amount of fibers is often spread in the base fluid to get the required outcomes without making the base fluid more viscous. The usefulness of fibers depends on maintaining a consistent fiber dispersion, which can be difficult in wellbore environments. To effectively use fibers in drilling and completion operations, a greater understanding of fiber suspension or stability in base fluids is required.²⁰ The efficiency of fibrous drilling sweeps in horizontal and severely deviated wells has been demonstrated in numerous investigations. Rheological characteristics of drilling fluids barely change when a trace amount of flexible monofilament fibers is added to them (concentrations less than 0.06 wt %). However, the rheological properties of drilling fluids containing fibers at concentrations higher than 0.09 wt % alter; a 0.4 wt % fiber addition to a hydroxypropyl guar gel resulted in a threefold increase in fluid viscosity.^{26–29} A small amount (0.02–0.04 wt

%) of fibers, when added to a dispersion of xanthan gum at a concentration of 0.35%, lowered the particle settling velocity by around 50%, according to an experimental study on spherical glass bead particles. Previous studies selected a fiber concentration range between 0.02 and 0.1%w to reduce settling velocity and ensure easy fluid pumping and processing.²⁹

2.3. Design of Experiments. The experimental design statistical technique, BBD, is employed to assess the multi-variable systems, examine the interaction impact of three variables, and enhance the responsiveness of multiple variable processes. The key benefit of the BBD methodology is that it requires fewer experimental trials than other approaches to analyze several factors.³⁰

This study examined three variables in water-based polymeric fluids with fiber lengths of 12 and 3 mm: base CMC concentration, fiber concentration, and cutting size (Table 2).

Table 2. Limits of the Studied Parameters^a

factors	symbol	factor levels		
		low (-1)	central (0)	high (+1)
cutting size (mm)	A	1	3.5	6
fiber (wt %)	B	0.02	0.06	0.1
CMC (wt %)	C	0.499	0.7495	1

^aTwo lengths of fibers: 3 and 12 mm.

For each fiber length, the BBD approach called for 45 sets of experimental trials (Table 3). A total of 96 experimental trials involving two fiber lengths were required. Experimental runs were randomized to reduce error and eliminate bias while maintaining the same settings.

The model of a *second-order polynomial equation* was generated as a response to the surface method Box–Behnken design and found to fit to a second-order polynomial with a regression coefficient of 0.99. The interaction between the variables and terminal velocity as a function of CMC concentration, fiber concentration, and cutting size are shown in eq 1.

$$V = n_0 + n_1A - n_2B - n_3C + n_4A^2 - n_5B^2 + n_6C^2 - n_7A \times B - n_8A \times C + n_9B \times C \quad (1)$$

A, *B*, and *C* are the three independent variables of the model; *A* is the cutting size; *B* is the fiber concentration; *C* is the polymer concentration; *V* is the response variable; n_0 is a model constant variable; n_1 , n_2 , and n_3 are linear coefficients; n_4 , n_5 , and n_6 represent the quadratic effects; and n_7 , n_8 , and n_9 indicate interaction effects of the model (see Table 4). The *P*-value states the significance of model-independent variables, where a *P*-value less than 0.05 means that the variable is significant.

2.4. Experimental Procedure. The required amount of CMC polymers was added to 50 L of tap water. The CMC was added gradually while being stirred at a gradually increasing stirring speed of up to 600 rpm for 3 h to prevent any aggregation, ensure quick mixing, and ensure the production of a homogeneous CMC fluid. The mixed CMC fluid was then left for 24 h for hydration. The next day, the mixed CMC was divided into containers to prepare 3 L of CMC fluid test samples. According to the experimental design, the required amounts of fibers were added to the samples gradually to prevent coagulation and ensure a homogeneous mixture formation. The required fibrous CMC fluid mixture was then transferred

Table 3. Three-Factor Box–Behnken Experimental Design for the 3 mm Fiber

run no.	cutting size (mm) (A)	fiber (wt %) (B)	CMC (wt %) (C)
1	1	-1	0
2	0	1	-1
3	-1	0	-1
4	1	0	-1
5	1	0	-1
6	-1	-1	0
7	-1	0	-1
8	-1	1	0
9	0	1	1
10	0	0	0
11	1	1	0
12	0	0	0
13	-1	-1	0
14	0	0	0
15	1	0	1
16	0	0	0
17	1	-1	0
18	0	-1	1
19	0	-1	-1
20	0	1	1
21	-1	0	1
22	0	0	0
23	0	0	0
24	0	0	0
25	-1	-1	0
26	0	1	-1
27	-1	0	1
28	1	1	0
29	0	-1	1
30	-1	1	0
31	1	0	1
32	0	-1	-1
33	0	-1	-1
34	1	1	0
35	1	-1	0
36	-1	1	0
37	0	1	1
38	0	-1	1
39	1	0	1
40	0	0	0
41	0	0	0
42	-1	0	1
43	0	1	-1
44	1	0	-1
45	-1	0	-1

into a cylindrical column of 53 cm height for measuring the suspension settling.

A photography unit composed of lighting, a high-speed video camera (FASTCAM SA3, Photron, Japan) which can capture up to 2000 pictures per second, and a PC was used to process the experimental data (see Figure 1). Particles were released from the top of the column one at a time, where photography lighting was used to monitor the particle motion, which is recorded by the camera. The PC was used to control the video camera and record the tracking profiles using Photron FASTCAM Viewer software 4 (PFV4) provided by Photron. The recorded particle motion is used to calculate the terminal velocity.

Table 4. *P*-Values and Regression Coefficients

term	3 mm length fiber V_1		12 mm length fiber V_2	
	<i>n</i> value	<i>P</i> -value	<i>n</i> value	<i>P</i> -value
n_0	4.405	0.000	4.106	0.000
n_1A	1.038	0.000	0.849	0.000
n_2B	10.77	0.000	13.63	0.000
n_3C	12.03	0.000	11.15	0.000
n_4A^2	0.071	0.000	0.071	0.000
n_5B^2	35.50	0.283	35.50	0.283
n_6C^2	7.433	0.000	7.433	0.000
$n_7A \times B$	1.537	0.001	1.537	0.001
$n_8A \times C$	1.178	0.000	1.178	0.000
$n_9B \times C$	21.83	0.000	21.83	0.000

It is worth mentioning that the normal classical equation for particle terminal velocity cannot be accommodated directly in these measurements because using different aspect ratios of fibers hinders the particles during the settling process and invalidates the concept of the classical terminal velocity formula. In addition, the classical formula is not applicable because the fluids tested in this are all non-Newtonian fluids, and the viscosity is a function of shear rate.

Tracker (a free video analysis and modeling tool from Open Source Physics, OSP) tracks the suspension cuttings independently by measuring the displacement in the vertical and horizontal axes with time, generating multiple variables such as velocity and acceleration. The settling time is calculated from the particle trajectory using the software. The tracking process starts by uploading the required experimental video recording to the tracker application, then defining the *X* and the *Y* axes, and setting the column's length. Also, we need to set the number of frames per second. Then, we define the tracking object by including its area inside the tracking circle to help the program track it easily with minor errors.

After tracking, five columns of data will be generated (Figure 2). An Excel sheet was used to define the terminal velocity for each trajectory and BBD to create a response surface regression for the experiment (Figure 3). The terminal velocity was calculated at a steady state using eq 2.

$$v_{\text{terminal}} = \frac{|y - y_0|}{t - t_0} \quad (2)$$

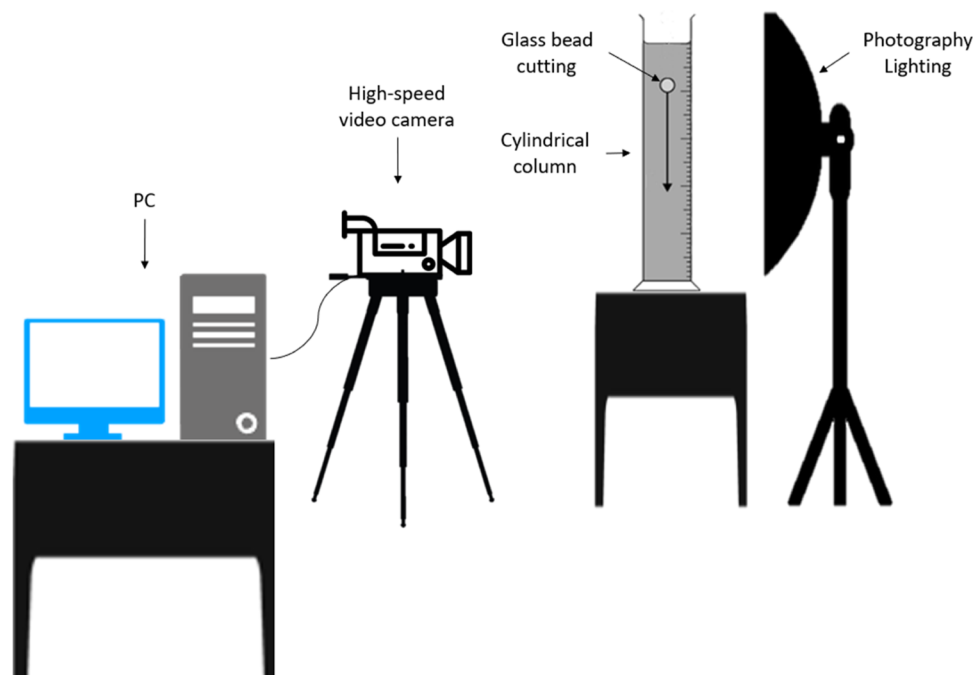
where y_0 is the initial particle displacement in cm at t_0 in seconds and y is the displacement in cm at any time t in seconds. A regression equation for cutting size, fiber wt %, and CMC wt % was generated for each fiber length. Using the SigmaPlot program, the 3 and 12 mm fiber length regression equations were used to plot 3D figures for interaction between design parameters.

A rheometer is used to test CMC rheological behavior. Experiments were carried out using an Anton Paar Modular Compact Rheometer (MCR) 302 Rheometer utilizing a Couette cell with 24 and 30 mm diameter and length, respectively. The shear rate varied from 0.01 to 100 s^{-1} , and the measurements were performed at room temperature (20 ± 1 $^{\circ}\text{C}$).

3. RESULTS AND DISCUSSION

3.1. Rheological Behavior. Studying the base CMC fluids' rheology is essential to understand better their solid carrying capacity and hydrodynamics. The shear rate was restricted to 1–100 s^{-1} . Over the full range of shear rates, the apparent fluid viscosity increased with the increase in polymer concentration from 0.5 to 1 wt %. Both concentrations of polymeric suspensions exhibit significant shear thinning.

Based on the low shear rate data extrapolation, the yield stress term is derived from the *y*-intercept of the linearized equation of shear stress vs. shear rate plot with the coefficient of determination R^2 (Table 5). The yield stress, which measures the maximum amount of tension that fluid can endure before

**Figure 1.** Experimental setup.

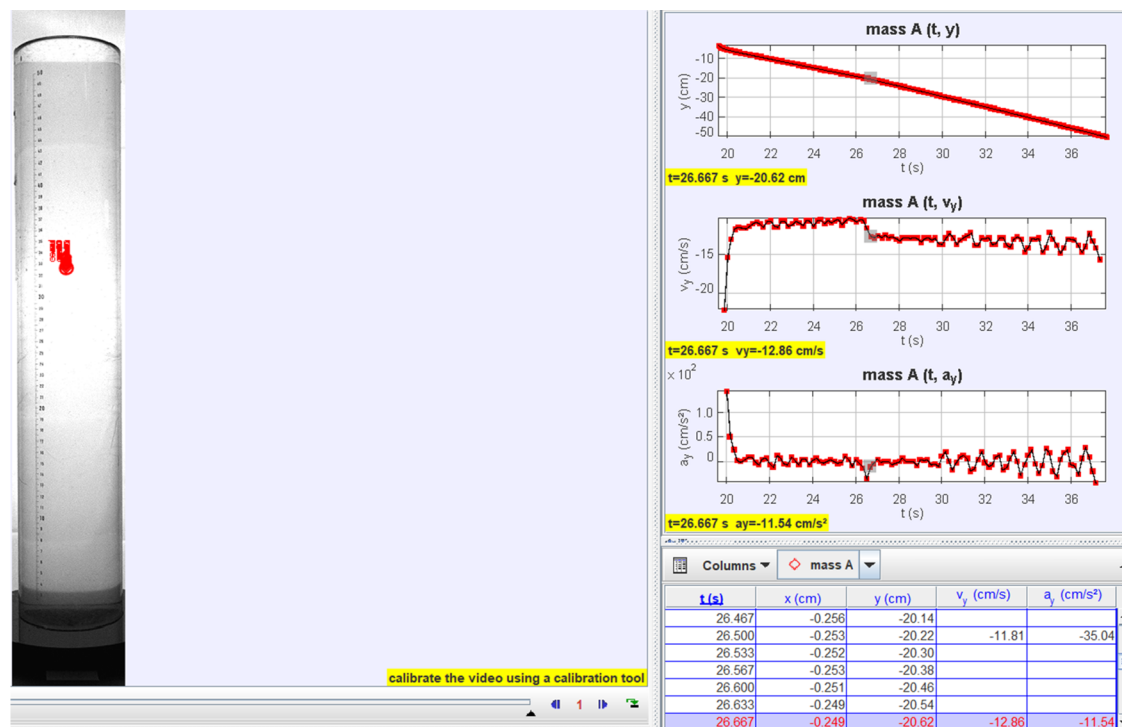


Figure 2. Experiment tracking and analysis using Tracker software.

Box-Behnken Design

WORKSHEET 1

Box-Behnken Design

Design Summary

Factors: 4 Replicates: 3
 Base runs: 30 Total runs: 90
 Base blocks: 1 Total blocks: 1

Center points: 18

+	C1	C2	C3	C4	C5	C6	C7	C8-T	C9	C10-T
	StdOrder	RunOrder	PtType	Blocks	Cutting Size	Fiber con%	Solution con%	Fiber length	Terminal V	
1	32	1	2	1	6.0	0.02	0.7495	3 mm	2.56542	Missing
2	85	2	2	1	3.5	0.10	0.4990	12 mm	0.85980	Missing
3	60	3	0	1	3.5	0.06	0.7495	12 mm	0.44811	Missing
4	70	4	2	1	3.5	0.10	0.4990	3 mm	1.88595	Missing
5	77	5	2	1	6.0	0.02	0.7495	12 mm	2.05071	Missing
6	76	6	2	1	1.0	0.02	0.7495	12 mm	0.08431	Missing
7	87	7	2	1	3.5	0.10	1.0000	12 mm	0.13768	Missing
8	26	8	2	1	3.5	0.02	1.0000	12 mm	0.26935	Missing
9	18	9	2	1	1.0	0.10	0.7495	12 mm	0.03759	Missing
10	35	10	2	1	1.0	0.06	0.4990	3 mm	0.29709	Missing
11	66	11	2	1	6.0	0.06	0.4990	3 mm	5.20634	Missing
12	36	12	2	1	6.0	0.06	0.4990	3 mm	5.23919	Missing
13	61	13	2	1	1.0	0.02	0.7495	3 mm	0.10863	Missing
14	30	14	0	1	3.5	0.06	0.7495	12 mm	0.46000	Missing

Figure 3. BBD design from Minitab.

Table 5. Power Law and Cross Model Fitted Data

CMC wt %	power law			cross model			
	τ_0 (mPa)	k (mPa·s)	R^2	η_0 (mPa·s)	η_∞ (mPa·s)	n	k (mPa·s)
0.5	5.0	88.5	0.99	94.6	1.1×10^{-5}	1.1	0.03
0.75	37.8	273.1	0.99	346.9	3.2×10^{-5}	0.6	0.03
1	217.6	741.2	0.99	1180.9	3.1×10^2	0.7	0.2

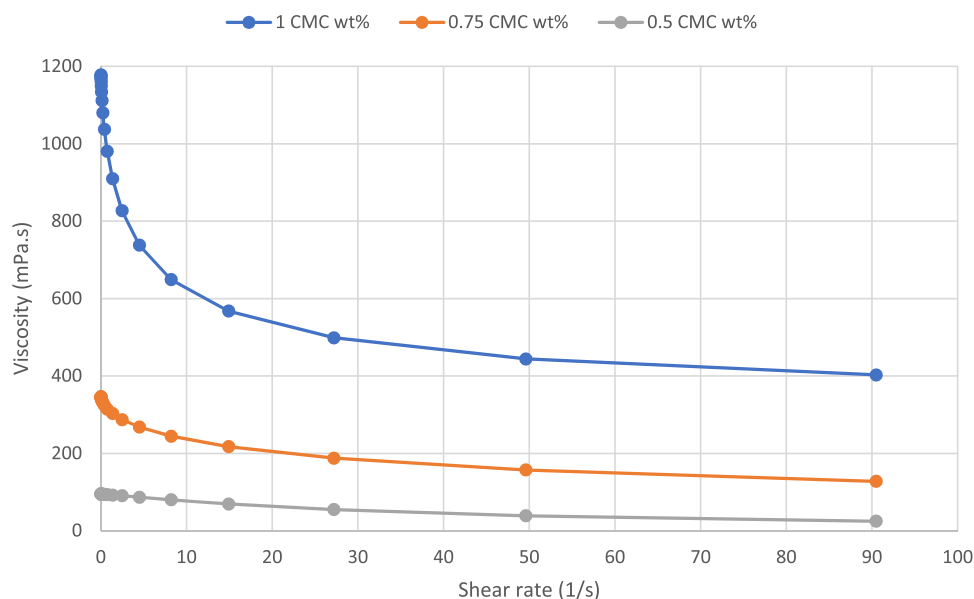


Figure 4. Viscosity of different CMC solutions vs shear rate.

yielding, is an essential factor.^{31,32} The power law model represents the linearized equation of the low shear rate data (eq 3).

$$\tau = \tau_0 + k\dot{\gamma} \quad (3)$$

where τ_0 is the yield stress, k is the consistency index, and $\dot{\gamma}$ is the shear rate.

The Cross model was also used to describe the rheological behavior of the CMC solution (eq 4)

$$\eta(\dot{\gamma}) = \frac{\eta_0 - \eta_\infty}{1 + (k\dot{\gamma})^n} + \eta_\infty \quad (4)$$

where $\eta(\dot{\gamma})$ is the viscosity as a function of shear rate and η_0 , η_∞ , k , and n are coefficients. The zero-shear viscosity η_0 is approached at very low shear rates, while the infinite shear viscosity η_∞ is approached at high shear rates.

Figure 4 shows the non-Newtonian behavior of different concentrations of CMC solutions. The non-Newtonian behavior of the CMC solutions is fitted using the power law and cross model (eq 4), and the results are summarized in Table 5.

3.2. Regression Modeling. Experimental design for the 3 mm length fiber results in terminal velocity values shown in Table 6. A second-order polynomial regression model investigated the link between the three parameters and the terminal velocities V_1 and V_2 for the 3 and 12 mm length fibers.

The outcomes of the terminal velocity regression equation for 3 and 12 mm are displayed in eqs 4 and 5, respectively.

$$V_1 = 4.405 + 1.0380A - 10.77B - 12.03C + 0.07129A^2 - 35.5B^2 + 7.433C^2 - 1.537A \times B - 1.1776A \times C + 21.83B \times C \quad (5)$$

$$V_2 = 4.106 + 0.8494A - 13.63B - 11.15C + 0.07129A^2 - 35.5B^2 + 7.433C^2 - 1.537A \times B - 1.1776A \times C + 21.83B \times C \quad (6)$$

The coefficients and their signs in eqs 1, 5, and 6 are generated by the software. Coefficients with positive signs show synergistic effects, whereas coefficients with negative signs indicate a negative impact on the stability response.³³ Therefore, terms with positive signs positively impact terminal velocity, whereas the ones with negative signs have the opposite effect. For instance, the quadratic terms A^2 , C^2 , and $B \times C$ and the linear term A in eq 4 all have positive signs, indicating that they influence the terminal velocity. The stability of the response decreases when other coefficients have negative signs, such as the first-order terms B and C and second-order terms B^2 , $A \times B$, and C .

The significance of coefficients and the impact of the interaction's combined terms are assessed using the probability P -value. P -values smaller than 0.05 indicate that a coefficient is more likely to affect the response significantly.^{34,35} The regression terms and accompanying P -values are displayed in Table 5. The V model indicates that every term is meaningful, except B^2 , which may be excluded without changing the model's prediction. The coefficient of determination, or R^2 , represents the proportion of variation in the dependent variable (V). The R^2 value indicates strong links between independent and

Table 6. BBD Terminal Velocity Response Data for the 3 mm Length Fiber

run order	cutting size (mm)	fiber (wt %)	CMC (wt %)	terminal V (cm/s)
1	6	0.02	0.7495	2.565
2	3.5	0.1	0.499	1.886
3	1	0.06	0.499	0.297
4	6	0.06	0.499	5.206
5	6	0.06	0.499	5.239
6	1	0.02	0.7495	0.109
7	1	0.06	0.499	0.291
8	1	0.1	0.7495	0.067
9	3.5	0.1	1	0.256
10	3.5	0.06	0.7495	0.809
11	6	0.1	0.7495	2.140
12	3.5	0.06	0.7495	0.805
13	1	0.02	0.7495	0.109
14	3.5	0.06	0.7495	0.805
15	6	0.06	1	1.933
16	3.5	0.06	0.7495	0.807
17	6	0.02	0.7495	2.565
18	3.5	0.02	1	0.305
19	3.5	0.02	0.499	2.680
20	3.5	0.1	1	0.257
21	1	0.06	1	0.060
22	3.5	0.06	0.7495	0.803
23	3.5	0.06	0.7495	0.814
24	3.5	0.06	0.7495	0.799
25	1	0.02	0.7495	0.109
26	3.5	0.1	0.499	1.903
27	1	0.06	1	0.064
28	6	0.1	0.7495	1.960
29	3.5	0.02	1	0.297
30	1	0.1	0.7495	0.069
31	6	0.06	1	2.067
32	3.5	0.02	0.499	2.565
33	3.5	0.02	0.499	2.622
34	6	0.1	0.7495	2.050
35	6	0.02	0.7495	2.433
36	1	0.1	0.7495	0.068
37	3.5	0.1	1	0.255
38	3.5	0.02	1	0.312
39	6	0.06	1	1.950
40	3.5	0.06	0.7495	0.813
41	3.5	0.06	0.7495	0.807
42	1	0.06	1	0.065
43	3.5	0.1	0.499	1.868
44	6	0.06	0.499	5.223
45	1	0.06	0.499	0.294

dependent variables. Accordingly, the model correlation has strong fitting values, with an R^2 value of 0.97.

3.3. Model Validation. Good model prediction versus experimental runs is observed in models V_1 and V_2 . Equation 4 for the 3 mm fibers and eq 5 for the 12 mm fibers were used to predict the terminal velocity. The observed and predicted terminal velocities of the suspended particles and the related error percentages are given in Table 7. The results show that most points are within a 30% error margin, indicating excellent agreement between experimental and anticipated values. The lowest error values for model V_1 are shown at point II, and when the fiber weight percent approaches the upper restrictions (+1) of components, the error rises rapidly. Although model V_2 shows

Table 7. Experimental Value Confirmation

parameters	0.02 fiber wt %, 3.5 mm cutting size		0.06 fiber wt %, 3.5 mm cutting size		0.1 fiber wt %, 3.5 mm cutting size	
	0.5 CMC wt %	1 CMC wt %	0.75 CMC wt %	1 CMC wt %	0.5 CMC wt %	1 CMC wt %
3 mm Fibers (V_1)						
experimental value	2.62	0.30	0.81	1.89	0.26	
model prediction	2.58	0.30	0.86	1.83	0.41	
error%	1.5	0	6.2	3.2	57	
12 mm Fibers (V_2)						
experimental value	2.02	0.27	0.46	0.83	0.14	
model prediction	1.99	0.18	0.40	1.01	0.06	
error%	1.5	33	13	22	57	

the same manner of error increment with fiber weight percent, it clearly shows a high error ratio compared to model V_1 . This may be because of the 12 mm fiber tendency to form a structured network²³ that blocks the path of the suspended cuttings and causes unpredictable trend.

3.4. Response Surface Analysis. 3D response surface plots were used to describe the regression equations that predicted the impact of cutting size, fiber (wt %), and CMC (wt %) on the terminal velocity of the cutting. The response surface plots were generated by changing two different independent variables and keeping the third independent variable constant, and the results are shown in Figure 5.

Minimizing the terminal velocity is the ultimate objective of this study. The Pareto chart in Figure 6 shows the significant effect of independent factors on the dependable factor (terminal velocity). In contrast to the impacts of cutting size and CMC concentration, fiber concentration and fiber length effects are insignificant (Figure 6); decreasing the cutting size or increasing polymer concentration significantly decreases terminal velocity. Although CMC concentration substantially affects the terminal velocity, cutting size has a more significant impact. The effect of reducing the terminal velocity with increasing CMC concentration is because of the relatively significant change in the viscosity (Figure 4). Another observation that could be inferred from Figure 5 is the different effect of increasing cutting size versus increasing fiber length from 3 to 12 mm.

Figure 5 also shows the combined impact of the two factors on the terminal velocity. It clearly illustrates that combining CMC wt % with cutting size shows the most significant effects among other factors. However, fiber weight and length affect the terminal velocity, and the combination of the fiber weight and fiber type, as well as duplication of the fiber weight, have no effect (Figure 6).

A perfect drilling fluid preparation factor ratio could be selected using contour plots (Figure 7) within the zone where the cutting terminal velocity is between 0 and 0.5 cm/s. Figure 7c shows that the region where CMC wt % is larger than 0.9 CMC wt % and cutting size equal to or smaller than 3.5 mm could be set as a perfect preparation range. Figure 7 also shows two other ranges, as shown in Figure 7a,b. We conclude from contour plots that fiber wt % has minor impacts on the terminal velocity, as drilling fluid preparation regions do not change with fiber wt % (Figure 7a,c).

Figure 8 illustrates design-independent factors' interaction with the cuttings' terminal velocity. When cutting size interacts

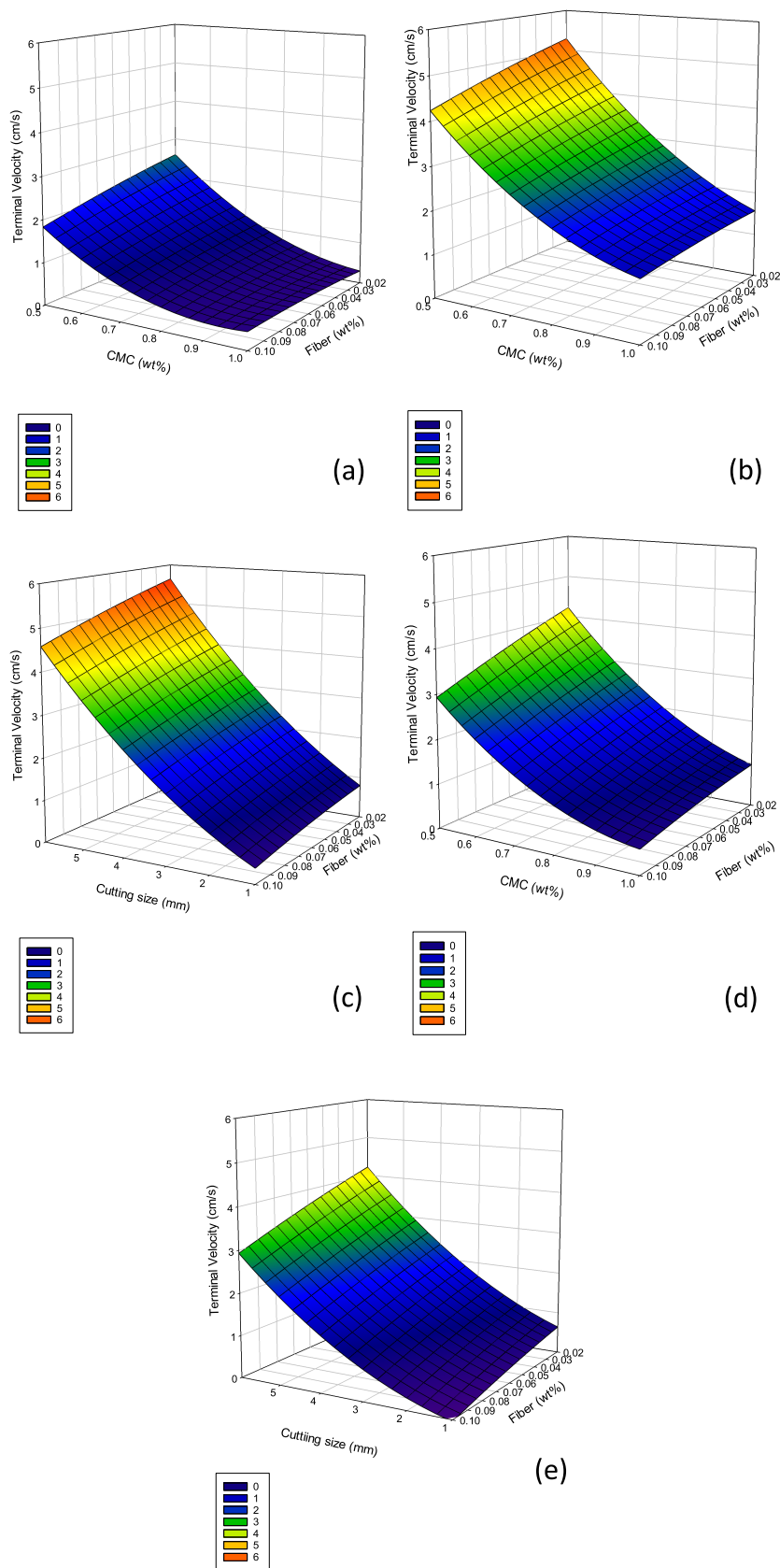


Figure 5. For 3 mm fibers, panels (a, b) show the effects of CMC wt % and fiber wt % for 3.5 and 6 mm cutting sizes, respectively, (c) shows the effects of cutting size and fiber wt % for 0.499 CMC wt %. For 12 mm fiber, panels (d, e) show the effects of CMC wt % and fiber wt % for 3.5 and 6 mm cutting sizes.

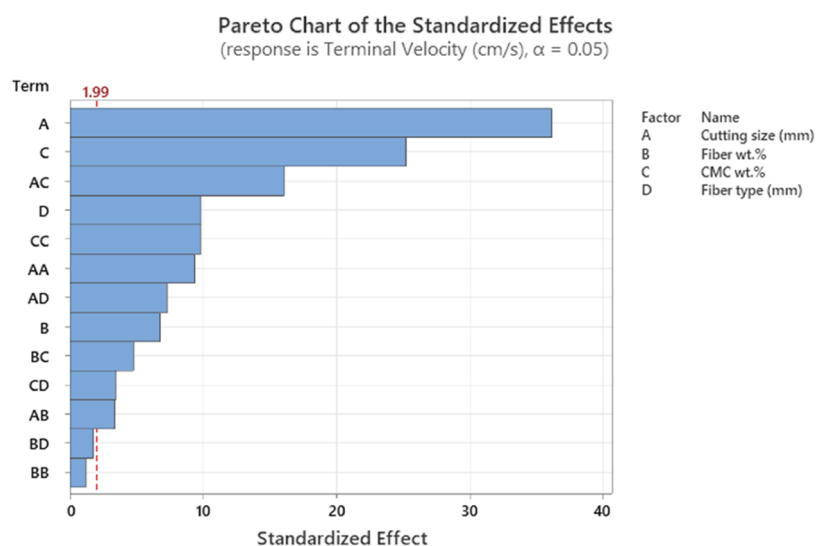


Figure 6. Pareto chart of the standardized effects.

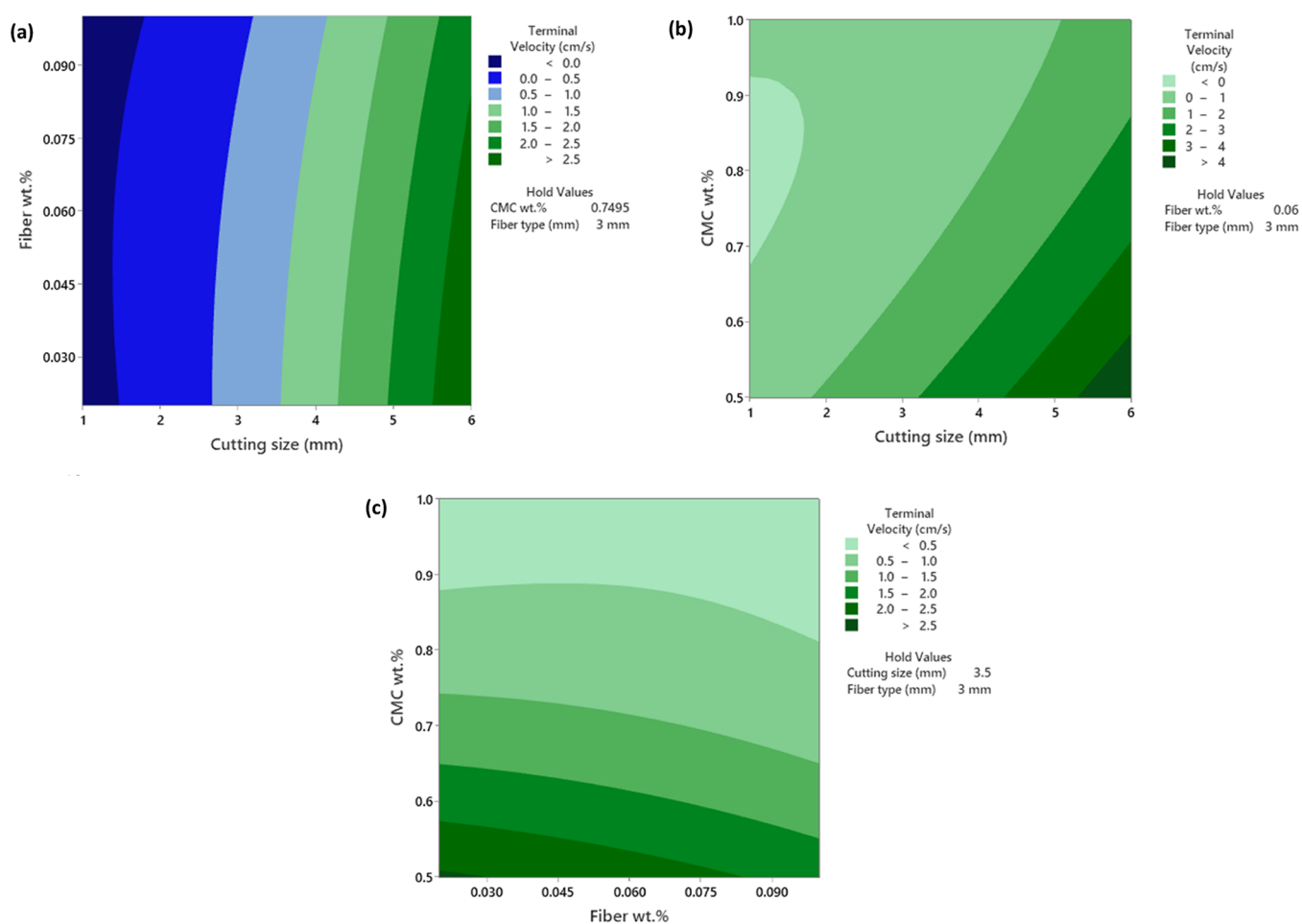


Figure 7. Contour plots for terminal velocity ranges for the 3 mm fiber: (a) fiber wt % vs cutting size with constant 0.75 CMC wt %, (b) CMC wt % vs cutting size with constant 0.06 fiber wt %, and (c) CMC wt % vs fiber wt % with constant 3.5 mm cutting size.

with other factors, the mean terminal speed is high. This is especially true when cutting size interacts with CMC concentration. This shows that cutting size is the most important factor on its own and with CMC concentration. Figure 6 could be used to reach the same conclusion.

3.5. Response Surface Optimization. Another technique for analyzing the optimization response surface is the desirability function. The response's projected values are converted into a dimensionless scale called d . The range of the desirability function is between $d = 0$ and $d = 1$, where $d = 0$ denotes undesirable response values and $d = 1$ denotes an entirely

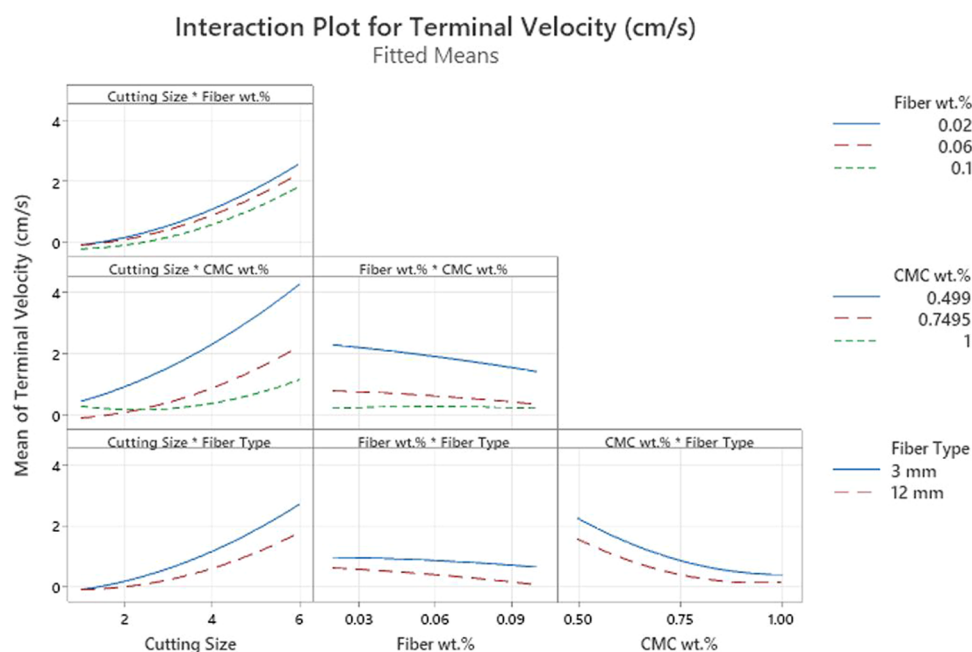


Figure 8. Design factor interaction plot.

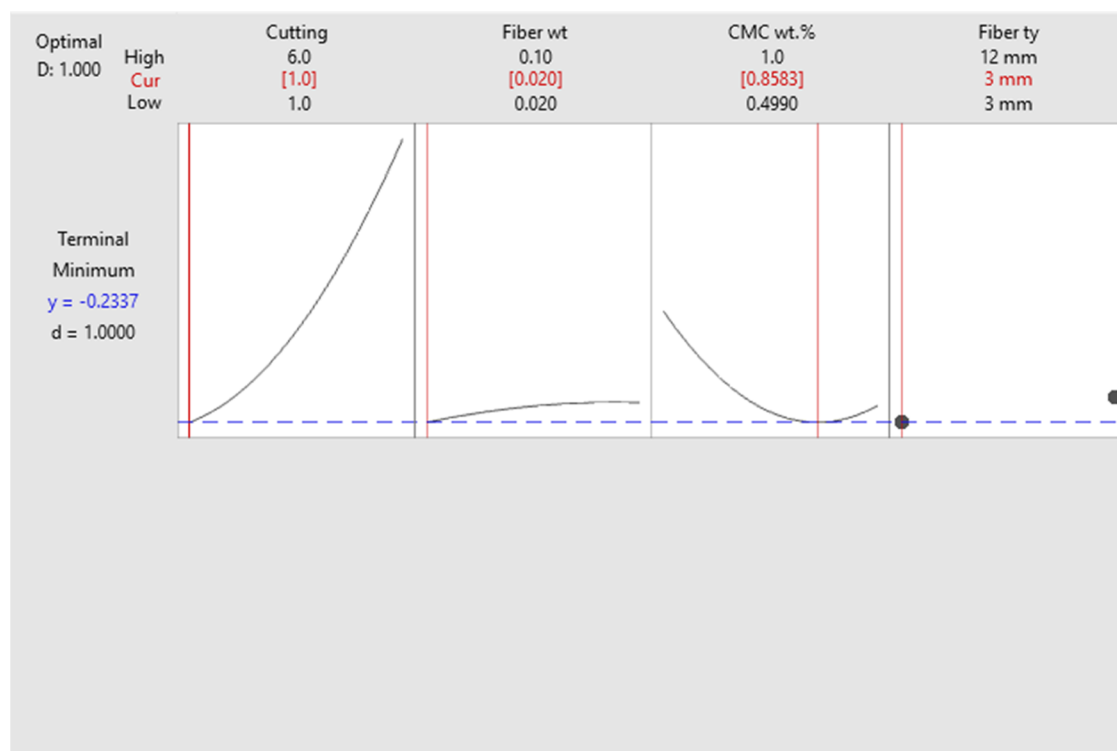


Figure 9. Optimization response.

desirably response.³⁶ By focusing on reducing the terminal velocity, the optimization was finished.

All desirability values met the desired minimum terminal velocity and were acceptable ($d = 1$). According to response data, the final terminal velocity is dominated by cutting size. The variables affecting the optimization of terminal velocity are shown in Figure 9. The vertical straight line shows the chosen factor level for each factor, and the horizontal dotted line represents the anticipated response value.

4. CONCLUSIONS

In this work, the terminal velocity of drilling cuttings was examined utilizing the Box–Behnken design with three replicates to derive models of the terminal velocity as a function of cutting size, CMC concentration, and fiber concentration. The terminal velocity was investigated using three cutting sizes of 1, 3.5, and 6 mm, three fiber concentrations of 0.02, 0.06, and 0.1 wt %, and two fiber lengths of 3 and 12 mm in a water-based drilling fluid of three CMC polymeric concentrations of 0.499, 0.7495, and 1 wt %. Models demonstrated that cutting size and

polymer concentration influenced the terminal velocity the most.

The following is a summary of the main findings:

- Cutting size represents the most important factor affecting the terminal velocity of the cuttings.
- Higher polymer concentrations improve fluid viscosity and decrease the terminal velocity of cuttings. At low polymer concentrations, the effects of fiber concentration on fluid viscosity are more noticeable; increasing the fiber concentration increases the fluid viscosity and creates networks that could hinder the settling. As a result, the impact of fiber concentration is correlated to polymer concentration.
- The combination of cutting size and CMC concentration results in a significant interaction.
- CMC fluids with a viscosity of 630.4 cP are sufficient to maintain a minimum terminal velocity of 0.234 cm/s with a cutting size of 1 mm and a fiber concentration of 0.02 of the 3 mm length fiber.

AUTHOR INFORMATION

Corresponding Author

Mustafa S. Nasser – Gas Processing Center, College of Engineering, Qatar University, 2713 Doha, Qatar; Department of Chemical Engineering, College of Engineering, Qatar University, 2713 Doha, Qatar; orcid.org/0000-0002-7646-558X; Email: m.nasser@qu.edu.qa

Authors

Arafat A. A. Mohammed – Gas Processing Center, College of Engineering, Qatar University, 2713 Doha, Qatar

Mohammed Alhajabdalla – Gas Processing Center, College of Engineering, Qatar University, 2713 Doha, Qatar; orcid.org/0000-0001-7725-8120

Husameldin Mahmoud – Gas Processing Center, College of Engineering, Qatar University, 2713 Doha, Qatar; orcid.org/0000-0002-0123-6643

Ibnelwaleed A. Hussein – Gas Processing Center, College of Engineering, Qatar University, 2713 Doha, Qatar; Department of Chemical Engineering, College of Engineering, Qatar University, 2713 Doha, Qatar; orcid.org/0000-0002-6672-8649

Ramadan Ahmed – The University of Oklahoma, Norman, Oklahoma 73019, United States

Complete contact information is available at:

<https://pubs.acs.org/10.1021/acsomega.3c01505>

Notes

The authors declare no competing financial interest.

ACKNOWLEDGMENTS

This work was made possible by the support of a National Priorities Research Program (NPRP) grant from the Qatar National Research Fund (QNRF) (grant reference number NPRP12S-0130-190023). The statements made herein are solely the responsibility of the authors. Open access funding is provided by the Qatar National Library.

REFERENCES

- (1) Dvoynikov, M. V.; Nutskova, M. V.; Blinov, P. A. Developments made in the field of drilling fluids by Saint Petersburg mining University. *Int. J. Eng., Trans. A* **2020**, *33*, 702–711.
- (2) Gandhi, S. M.; Sarkar, B. C. Drilling. In *Essentials of Mineral Exploration and Evaluation*; Elsevier, 2016; pp 199–234.
- (3) Magzoub, M. I.; Shamlooh, M.; Salehi, S.; Hussein, I.; Nasser, M. S. Gelation kinetics of PAM/PEI based drilling mud for lost circulation applications. *J. Pet. Sci. Eng.* **2021**, *200*, No. 108383.
- (4) Elgaddafi, R.; Ahmed, R.; Karami, H.; Nasser, M.; Hussein, I. A Mechanistic Model for Wellbore Cleanout in Horizontal and Inclined Wells. *SPE Drill. Completion* **2021**, *36*, 832–848.
- (5) Antia, M.; Ezejiakor, A. N.; Obasi, C. N.; Orisakwe, O. E. Environmental and public health effects of spent drilling fluid: An updated systematic review. *J. Hazard. Mater. Adv.* **2022**, *7*, No. 100120.
- (6) Fagundes, K. R. S.; da Souza Luz, R. C.; Fagundes, F. P.; de Carvalho Balaban, R. Effect of carboxymethylcellulose on colloidal properties of calcite suspensions in drilling fluids. *Polimeros* **2018**, *28*, 373–379.
- (7) Neff, J. M. Biological Effects of Drilling Fluids, Drill Cuttings and Produced Waters. In *Long-term Environmental Effects of Offshore Oil and Gas Development*; CRC Press, March 24, 1987; pp 479–548.
- (8) Magzoub, M. I.; Salehi, S.; Hussein, I. A.; Nasser, M. S. Investigation of Filter Cake Evolution in Carbonate Formation Using Polymer-Based Drilling Fluid. *ACS Omega* **2021**, *6*, 6231–6239.
- (9) Awad, A. M.; Hussein, I. A.; Nasser, M. S.; Karami, H.; Ahmed, R. CFD modeling of particle settling in drilling fluids: Impact of fluid rheology and particle characteristics. *J. Pet. Sci. Eng.* **2021**, *199*, No. 108326.
- (10) Shamlooh, M.; Hamza, A.; Hussein, I.; Nasser, M.; Salehi, S. In *Gelation Performance of PAM/PEI Polymer-Based Mud System for Lost Circulation Control*, 27th European Meeting of Environmental and Engineering Geophysics, Held at Near Surface Geoscience Conference and Exhibition 2021, NSG 2021, 2021, Vol. 2021, pp 1–5.
- (11) Elgaddafi, R.; Ahmed, R.; Growcock, F. Settling behavior of particles in fiber-containing Herschel Bulkley fluid. *Powder Technol.* **2016**, *301*, 782–793.
- (12) Ezeakacha, C. P.; Salehi, S. Experimental and statistical investigation of drilling fluids loss in porous media—part 1. *J. Nat. Gas Sci. Eng.* **2018**, *51*, 104–115.
- (13) Razak Ismail, A.; Seong, T. C.; Buang, N. A.; Rosli, W.; Sulaiman, W. Improve Performance of Water-based Drilling Fluids. *Sriwijaya Int. Semin. Energy Environ. Sci. Technol.* **2014**, *1*, 43–47.
- (14) Busahmin, B.; Saeid, N. H.; Hasan, U. H. B. H.; Alusta, G. Analysis of Hole Cleaning for a Vertical Well. *Open Access Library J.* **2017**, *04*, No. 76215.
- (15) Rasi, M. In *Hole Cleaning in Large, High-Angle Wellbores*, Drilling Conference - Proceedings, Feb 15, 1994; pp 299–310.
- (16) Mohammadsalehi, M.; Malekzadeh, N. In *Optimization of Hole Cleaning and Cutting Removal in Vertical, Deviated and Horizontal Wells*, Society of Petroleum Engineers - SPE Asia Pacific Oil and Gas Conference and Exhibition 2011, 2011, Vol. 1, pp 301–308.
- (17) Ahmed, R. M.; Takach, N. E. Fiber Sweeps for Hole Cleaning. *SPE Drill. Completion* **2009**, *24*, 564–573.
- (18) Ozbayoglu, M. E.; Osgouei, R. E.; Ozbayoglu, M.; Yuksel, E. In *Estimation of Very-Difficult-to-Identify Data for Hole Cleaning, Cuttings Transport and Pressure Drop Estimation in Directional and Horizontal Drilling*, Society of Petroleum Engineers - IADC/SPE Asia Pacific Drilling Technology Conference 2010, Nov 1, 2010.
- (19) Evren, O. M.; Reza, O. E.; Murat, O. A.; Ertan, Y. In *Estimation of Very-Difficult-to-Identify Data for Hole Cleaning, Cuttings Transport and Pressure Drop Estimation in Directional and Horizontal Drilling*, Society of Petroleum Engineers - IADC/SPE Asia Pacific Drilling Technology Conference 2010, 2010; pp 668–685.
- (20) Alhajabdalla, M.; Mahmoud, H.; Nasser, M. S.; Hussein, I. A.; Ahmed, R.; Karami, H. Application of response surface methodology and box-behnken design for the optimization of the stability of fibrous dispersion used in drilling and completion operations. *ACS Omega* **2021**, *6*, 2513–2525.
- (21) Mahmoud, H.; Alhajabdalla, M.; Mohammed, A. A. A.; et al. Pilot-scale study on the suspension of drill cuttings: Effect of fiber and fluid characteristics. *J. Nat. Gas Sci. Eng.* **2022**, *101*, No. 104531.

(22) Mendez, M.; Garcia, S.; Ahmed, R.; Karami, H.; Nasser, M.; Hussein, I. In *Effect of Fluid Rheology on the Performance of Fibrous Fluid in Horizontal Well Cleanout*, Society of Petroleum Engineers - SPE/ICoTA Well Intervention Conference and Exhibition, CTWI 2022, March 15, 2022.

(23) Mahmoud, H.; Alhajabdalla, M.; Nasser, M. S.; Hussein, I. A.; Ahmed, R.; Karami, H. Settling behavior of fine cuttings in fiber-containing polyanionic fluids for drilling and hole cleaning application. *J. Pet. Sci. Eng.* **2021**, *199*, No. 108337.

(24) Yan, T.; Wang, K.; Sun, X.; Luan, S.; Shao, S. State-of-the-art cuttings transport with aerated liquid and foam in complex structure wells. *Renewable Sustainable Energy Rev.* **2014**, *37*, 560–568.

(25) Ford, J. T.; Peden, J. M.; Oyenyin, M. B.; Gao, E.; Zarrouh, R. Experimental Investigation of Drilled Cuttings Transport in Inclined Boreholes. *Delta* **1990**, 197–206.

(26) Guo, J.; Ma, J.; Zhao, Z.; Gao, Y. Effect of fiber on the rheological property of fracturing fluid. *J. Nat. Gas Sci. Eng.* **2015**, *23*, 356–362.

(27) Elgaddafi, R.; Ahmed, R.; Growcock, F. Settling behavior of particles in fiber-containing Herschel Bulkley fluid. *Powder Technol.* **2016**, *301*, 782–793.

(28) Jiang, Q.; Jiang, G.; Wang, C.; et al. The influence of fiber on the rheological properties, microstructure and suspension behavior of the supramolecular viscoelastic fracturing fluid. *J. Nat. Gas Sci. Eng.* **2016**, *35*, 1207–1215.

(29) Elgaddafi, R.; Ahmed, R.; George, M.; Growcock, F. Settling behavior of spherical particles in fiber-containing drilling fluids. *J. Pet. Sci. Eng.* **2012**, *84–85*, 20–28.

(30) Ferreira, S. L. C.; Bruns, R. E.; Ferreira, H. S.; et al. Box-Behnken design: an alternative for the optimization of analytical methods. *Anal. Chim. Acta* **2007**, *597*, 179–186.

(31) Sahu, K. C.; Valluri, P.; Spelt, P. D. M.; Matar, O. K. *Linear Instability of Pressure-Driven Channel Flow of a Newtonian and a Herschel-Bulkley Fluid*, 2007.

(32) Magzoub, M. I.; Kiran, R.; Salehi, S.; Hussein, I. A.; Nasser, M. S. Assessing the Relation between Mud Components and Rheology for Loss Circulation Prevention Using Polymeric Gels: A Machine Learning Approach. *Energies* **2021**, *14*, No. 1377.

(33) Khnifira, M.; Boumya, W.; Machrouhi, A.; et al. Box-Behnken design for the understand of adsorption behaviors of cationic and anionic dyes by activated carbon Box-Behnken design for understanding of adsorption behaviors of cationic and anionic dyes by activated carbon. *Desalin. Water Treat.* **2021**, 204–211.

(34) Singh, R.; Ahmed, R.; Karami, H.; Nasser, M.; Hussein, I. CFD Analysis of Turbulent Flow of Power-Law Fluid in a Partially Blocked Eccentric Annulus. *Energies* **2021**, *14*, No. 731.

(35) Awad, A. M.; Hussein, I. A.; Nasser, M. S.; Ghani, S. A.; Mahgoub, A. O. A CFD- RSM study of cuttings transport in non-Newtonian drilling fluids: Impact of operational parameters. *J. Pet. Sci. Eng.* **2022**, *208*, No. 109613.

(36) Ramasamy, R. R.; Amasamy, A.; Ra, R.; Avi, A. A. A.; Vi, V. I. *Simultaneous Optimization of a Multi-Response System by Desirability Function Analysis of Boondi-Making: A Case Study*, 2005; Vol. 70. www.ift.org.